Amelioration of depressive symptoms on Fawn-Hooded rats through the 'healthy' fecal microbiota transplantation

Bing Hu
Beijing Institute of Technology
Promi Das
University of California San Diego
Xianglin Lv
Peking University
Meng Shi
Peking University Hospital of Stomatology
Jiye Aa
China Pharmaceutical University
Kun Wang
Peking University Third Hospital
Liping Duan
Peking University Third Hospital
Jack Gilbert
University of California San Diego
Yong Nie
Peking University https://orcid.org/0000-0002-5940-1218
Xiao-Lei Wu (xiaolei_wu@pku.edu.cn)
Peking University https://orcid.org/0000-0002-9897-6903

Article

Keywords: Fecal microbiota transplantation, Depression remedy, Microbiota-gut-brain (MGB) axis, Metabolomics, Neuromodulation

Posted Date: September 25th, 2021

DOI: https://doi.org/10.21203/rs.3.rs-917357/v1

Abstract

Gut microbiome dysbiosis is associated with the development of depression. Fecal microbiota transplantation (FMT) has been proposed as a potential therapeutic solution for depression. However, the efficacy of FMT to reduce depression is still unknown. We performed FMT from Sprague-Dawley (SD) rats ('healthy' controls) to Fawn-hooded (FH) rats (depression model). Pre-FMT, the FH rats exhibited significantly elevated depressive behaviors and distinct neurotransmitter and cytokine levels compared with SD rats. Post-FMT, FH recipients receiving SD microbiota showed reduced depressive behaviors, a significant increase in hippocampal neurotransmitters and a significant decrease of some hippocampal cytokines compared to the ones receiving FH microbiota. SD-FMT resulted in the FH recipients' gut microbiome resembling the SD donor; additionally, FH recipients showed a significant shift in the serum metabolome, but not the hippocampal metabolome. Co-occurrence analysis suggests that SD-FMT ameliorated recipients' physiochemical features of depression by the metabolic modulation through the enteric nervous system, the intestinal barrier and the blood-brain barrier. Our results provided new data pointing to multiple mechanisms of interaction for the impact of gut microbiome modulation on depression.

Introduction

Depression is a recurrent, heterogeneous mood disorder, occurring in more than 260 million people worldwide[1]. Its etiology involves impaired regulatory mechanisms of neuroendocrine, immune, and neurotransmitter systems[2]. Although there has been little progress in the identification of biomarkers, much of the research converges on the decreased concentration of monoamine neurotransmitters (e.g., serotonin, noradrenaline, and dopamine) in the brain, atrophy of mature neurons in the hippocampus, or reduced neurogenesis in the hippocampus[3]. Clinical studies with chronically depressed patients have also demonstrated significantly increased proinflammatory cytokines, such as tumor necrosis factor (TNF)-α, interleukin (IL)-1β, and IL-6, which are immune communicators between the brain and the peripheral system[4], suggesting long-term impairment of neuroinflammatory molecules in the brain and blood.

Numerous studies have provided evidence suggesting a role for the gut microbiome and the associated metabolites in modulating neuro-biochemistry and behaviors through the microbiota-gut-brain (MGB) axis[5–7]. Studies in humans[8–10], macaques[11], and rodents[12] have demonstrated a variable microbial signature associated with major depressive disorder or similar depression-like phenotypes. The gut microbiome can also be used to transfer this phenotype between hosts, such that germ-free mice or antibiotic treated rats exhibited depression-like behaviors two weeks after they have been colonized with the fecal microbiota of depressed human patients[13,14].

Pioneering studies examining the relationship between the gut microbiota and major depressive disorder have suggested that a disrupted microbiome (dysbiosis) can directly increase intestinal permeability, y translocation of immune activators[15–18]. This immune

activation may also trigger alteration in neurotransmitter production[19–21], influencing brain activity and resulting in central nervous system (CNS) disorders[22]. However, the mechanisms remain elusive, and a lack of identified causality hinders the translation of preventive and therapeutic strategies to clinic.

Despite the lack of validated causal mechanisms, gut microbiome modulation has already been proposed as a potential therapeutic solution for depression[23,24]. Administration of the probiotic *Bifidobacterium longum* NCC3001 reduced both symptoms of irritable bowel syndrome (IBS) and depression in patients, potentially due to the reduction in limbic reactivity[25]. Daily administration of *Faecalibacterium prausnitzii* ATCC27766 for a period of four weeks significantly alleviated anxiety- and depression-like behaviors in rats, possibly via the regulation of host cytokine metabolism[26]. However, any beneficial effect of probiotic therapy might be transient. For instance, the anxiolytic and antidepressant-like effects of probiotic therapy lasted no more than two months in older adults[27]. This is likely driven by the resilience of the indigenous gut microbiota to the invasion of new species. Therefore, it is suggested that current psychobiotics may have limited potential to disrupt a depression-associated gut microbial ecosystem, unless more complex communities are used[28]. Manipulating the gut-brain axis of depression via fecal microbiota transplantation (FMT) has been explored by using the fecal matter of depressed donors into germ-free mice[29,30], but whether FMT from a 'healthy' donor can influence recipient depressive symptoms has yet to be explored.

Here, the impact of microbiome transfer from a conventional animal model, Sprague Dawley (SD) rats, to a genetically impaired animal model, Fawn-hooded (FH) rats which are known for their altered serotonergic activity[31], on the recipient's neurophysiology, immune profile, microbiome and behavior was determined. This model system was used to test the following hypotheses: (i) FMT would result in increased microbiome similarity between the recipient and the donor; (ii) the recipient's neurobehavioral, physiochemical, and immunological characteristics would be within the quantified ranges demonstrated by the donor following FMT. To test these hypotheses, fecal, serum and hippocampal tissue samples were collected from the experimental rat groups to characterize the fecal microbiome by metagenomics and to quantify the microbial metabolites in serum and hippocampal tissue by untargeted metabolomics and immunoassays. It was demonstrated that FMT from the 'healthy' SD model to the 'depressed' FH model resulted in significant changes in the microbiome, serum metabolome, hippocampal cytokine profiles and neurotransmitter levels, and behaviors in the FH recipients.

Results

Neurobehavioral and neurotransmitter characterization of the control and FMT-processed rats

To test if the neurobehavioral characteristics of the recipient FH rats upon FMT were altered toward the quantified range of the donor SD rats, three anxiety-like and depression-like behavioral tests, including the

est (OFT), and the sucrose preference test (SPT), were

conducted on all four groups of rats. As shown in Fig. 1a, FST scores were significantly different between FH and SD rats (two-tailed *t*-test, p = 0.0183), and FMT significantly reduced the floating time of FH recipients receiving SD fecal microbiota (FH-SD rats) in comparison to FH fecal microbiota recipients (FH-FH rats; two-tailed *t*-test, p = 0.0468). Figure 1b showed that FH and SD rats had significantly different OFT scores (two-tailed *t*-test, p = 0.0178), and FMT resulted in a non-significant trend toward an increase in the central to total movement ratio for FH-SD rats compared to FH-FH rats (two-tailed *t*-test, p = 0.0606). For SPT, the sucrose-preference index suggested a significant trend toward a greater sucrose preference in FH-SD rats compared to FH (two-tailed *t*-test, p = 0.0093) and FH-FH rats (two-tailed *t*-test, p = 0.0122; Fig. 1c). Altogether, these results indicated that FH-SD rats presented behaviors more like SD rats than FH or FH-FH rats, which suggested that FMT of the SD gut microbiome could be responsible for the behavioral shifts in recipients.

Similarly, to determine if the neurotransmitter concentrations in recipient FH rats upon FMT had altered toward those observed for donor SD rats, we measured three major neurotransmitters (i.e., serotonin, norepinephrine, and dopamine) in all four groups of rats. Owing to the genetic dysfunctional nature of the serotoninergic system in the FH rats, the serotonin concentrations in serum was significantly lower for FH rats (two-tailed test, $p = 1.9\times10^{-6}$), FH-FH rats (two-tailed test, $p = 2.1\times10^{-6}$) and FH-SD rats (two-tailed test, $p = 1.7\times10^{-6}$) than those for SD rats (Fig. 1d). However, the hippocampal concentrations of serotonin (Fig. 1e) were significantly higher in FH-SD rats than those in FH (two tailed *t*-test, p = 0.0379) and FH-FH rats (two tailed *t*-test, p = 0.0122), while they were similar with those in SD rats (two tailed *t*-test, p = 0.0715). One explanation of these results is that the transplantation of SD fecal microbiota to FH rats influenced neuromodulation through the enteric nervous system (ENS), not blood circulation. Norepinephrine (Fig. 1f) and dopamine (Fig. 1g) also had significantly higher hippocampal concentrations in FH-SD rats than FH (two tailed *t*-test, $p_{nor}= 0.0016$ and $p_{dop} = 0.0004$, respectively) and FH-FH rats (two tailed *t*-test, $p_{nor}=0.0081$ and $p_{dop} = 0.0022$, respectively). Considering that hippocampal norepinephrine concentrations in control SD rats were significantly higher than those in control FH rats (two tailed *t*-test, p = 0.0281), while they were similar with those in FH-SD rats (two tailed *t*-test, p = 0.5748), it was inferred that FMT of the SD microbiome ameliorated the situation of hippocampal norepinephrine reduction in FH rats. Interestingly, FH-SD rats showed a significant increase in hippocampal dopamine concentrations compared to SD rats (two tailed *t*-test, p = 0.0092; Fig. 1g), suggesting some unknown effect of FMT on this neurotransmitter.

Cytokine quantification in control and FMT-processed rats

To determine if FMT influenced immune responses in the rats, cytokines in both the serum and hippocampus of the control and FMT-processed rats were quantified. Serum cytokines IL-4 and IL-10 had significantly lower levels in FMT-processed rats compared to either FH (two tailed *t*-test, $p_{IL-4} = 0.0174$ and $p_{IL-10} = 0.0079$ for FH-FH rats; $p_{IL-4} = 1.2\times10^{-6}$ and $p_{IL-10} = 4.5\times10^{-7}$ for FH-SD rats) or SD rats (two tailed *t*-test, $p_{IL-4} = 0.0083$ and $p_{IL-10} = 0.0030$ for FH-FH rats; $p_{IL-4} = 0.0022$ and $p_{IL-10} = 1.3\times10^{-7}$ for FH-SD rats). However, most serum cytokine concentrations were not significantly different following FMT or

e levels of hippocampal cytokines IL-1b and TNF-α were

significantly lower in SD rats than FH rats (two tailed *t*-test, p_{IL-1b} = 0.0356 and $p_{TNF-\alpha}$ = 0.0028, respectively), and they showed a non-significant trend toward lower levels in FH-SD rats compared to FH-FH rats (two tailed *t*-test, p_{IL-1b} = 0.1739 and $p_{TNF-\alpha}$ = 0.0598, respectively; **Fig. S1**). Interestingly, hippocampal IL-17A contents in FH-FH rats were significantly higher than that in FH (two tailed *t*-test, p = 0.0123) and FH-SD rats (two tailed *t*-test, p = 0.0052), suggesting that FH microbiome transplantation could induce IL-17A accumulation in FH rat hippocampus. All above results indicated that SD microbiome transplantation could induce a decrease of some hippocampal immune cytokines in FH recipients.

FMT-mediated changes in fecal microbial taxonomy

To determine if the gut microbiota in FH-SD rats had been altered, species-level beta-diversity based on 16S rRNA amplicon sequencing data was analyzed using DEICODE. As shown in Fig. 2a, FH and FH-FH rats had significantly different beta diversity compared to FH-SD and SD rats (PERMDISP: F-statistic 0.230, p-value 0.818, n = 999 permutations; PERMANOVA: F-statistic 8.689, p-value 0.001, n = 999 permutations). The SD microbiota was significantly differentiated from the FH microbiota by the proportion of *Roseburia* sp. CAG 380 and *Dialister* sp. CAG: 357. Likewise, the FH microbiota was characterized by increased proportions of *Bifidobacterium pseudolongum* and *Candidatus* Gastranaerophilus phascolarctosicola. Log-ratio of DEICODE-feature loadings of these four species were employed further to examine the proportion of SD:FH-associated species. A significantly greater log-ratio of *Roseburia* sp. CAG 380 and *Dialister* sp. CAG: 357 (in the numerator) to *Bifidobacterium pseudolongum* and *Candidatus* Gastranaerophilus phascolarctosicola (in the denominator) between FH and SD control groups, as well as between FH-FH and FH-SD rats, were observed (Mann-Whitney Wilcox test, $p < 0.05$; **Fig. S2**). This suggested a successful transfer of the SD gut microbiota to the FH recipient rats. To further identify differentially proportional taxa and account for the compositional data, ANCOM-BC was applied. As shown in Fig. 2b, there were eight species with significantly different proportions both between the two control groups (i.e., SD vs FH) and between the two FMT-processed groups (i.e., FH-FH vs FH-SD) (effect sizes with Bonferroni-adjusted $p < 0.05$). These differentially proportional species were *Akkermansia muciniphila*, *Akkermanisia muciniphila* CAG:154, *Bifidobacterium adolescentis*, *Dialister* sp. CAG357, *Firmicutes bacterium* CAG:41, *Ruminococcus* sp. CAG:108, *Sutterella wadsworthensis* CAG:135, *Veillonella* sp. ACP1, and their proportions were significantly lower in SD and FH-SD rats than in FH and FH-FH rats. Interestingly, *Dialister* sp. CAG357 was the sole pairwise differentially proportional species that could determine the species-level beta-diversity differentiation between SD and FH-SD gut microbiota and the FH and FH-FH gut microbiota (Fig. 2a). Therefore, it was considered that the SD fecal microbiota transplantation was successful in shifting the microbiota of the recipient FH rats towards the SD-characteristic microbiota, and the significant decrease of *Dialister* sp. CAG357 might play a key role in the gut microbiota reassembly in FH-SD rats.

FMT-mediated changes in fecal microbial functional potential

To determine if the genetic functional potential of the recipient FH rat microbiome was altered by the donor SD rat microbiome upon FMT, MetaCyc database-mapped enzymatic reactions and pathways for the metagenomic data of the four groups were analyzed using DEICODE beta-diversity. As shown in Fig. 3a, FH and FH-FH rats had significantly different beta-diversities compared to FH-SD and SD rats in terms of enzymatic reactions (PERMDISP: F-statistic 1.420, p-value 0.179, n = 999 permutations; PERMANOVA: F-statistic 7.155, p-value 0.001, n = 999 permutations). It was found that the group of SD and FH-SD microbiomes was characterized by the gene encoding 1-deoxy-D-xylulose 5-phosphate reductoisomerase, while the clustering of FH and FH-FH microbiomes was characterized by genes encoding citrate hydro-lyase, D-threo-isocitrate hydro-lyase, sucrose phosphorylase, acetolactate synthase, butyryl-CoA dehydrogenase, isoamylase, and phosphoglucomutase. Similar to the taxonomic beta-diversity analysis, the functional beta-diversity in FH-SD rats was more similar to SD rats than to FH and FH-FH rats (**Fig S3a**). The metabolic pathways that defined the SD and FH-SD microbiomes were quinate degradation I and II, gallate biosynthesis, urea cycle, and carbamoyl-phosphate synthesis, while the pathways that characterized the FH and FH-FH microbiomes were L-citrulline biosynthesis, L-citrulline degradation, and L-proline biosynthesis II (from arginine). Quinate was one of several aromatic compounds that can be metabolized by microorganisms to the central intermediate protocatechuate and then be further metabolized via the β-ketoadipate pathway to acetyl-CoA and succinyl-CoA. According to a Spearman's rank correlation analysis between the robust-Aitchison (RPCA) generated distance-ordination matrices of functional genes at the reaction level (along the X-axis) and pathway level (along the Y-axis), it was demonstrated that there was a significant association between the pathways and enzyme reactions with $\rho = 0.8741$ (over 999 permutations, p-value = 0.001; **Fig. S3b**). By applying ANCOM-BC, the pairwise differentially proportional enzyme-encoding genes and pathways in both the control groups (i.e., SD vs FH) and FMT-processed groups (i.e., FH-FH vs FH-SD) were identified. Nine metabolic pathways were pairwise differentially proportional, including glycolipid biosynthesis, chondroitin sulfate degradation, CMP-legionaminate biosynthesis, dermatan sulfate degradation, pyruvate fermentation – acetoin I, pyruvate fermentation – acetoin, starch degradation II, and zwittermicin A biosynthesis (**Fig S3c**). As shown in Fig. 3b, there were 29 pairwise differentially abundant enzyme genes, all of which were significantly less abundant in SD or FH-SD microbiomes than those in FH or FH-FH microbiomes, respectively (effect sizes with Bonferroni-adjusted $p < 0.05$). Most of the pairwise differentially abundant genes were associated with carbon metabolism. Among them, the gene encoding acetolactate synthase, which could catalyze the conversion between pyruvate and 2-acetolactate and was involved in valine and isoleucine biosynthesis and then pantothenate and CoA biosynthesis, was the only one associated with the beta-diversity differentiation between SD/FH-SD and FH/FH-FH (Fig. 3a). Hence, SD-FMT significantly changed the microbiome profile of FH rats, resulting in a significant reduction in the proportion of genes encoding acetolactate synthase.

Microbe-metabolite co-occurrences amongst the group-associated features

Serum and hippocampal metabolomics were performed for the four groups of rats. Comparative

erum metabolomic profiles were relatively conserved between

all four rat groups (Fig. 4a-b), but hippocampal metabolite profiles were considerably different between control rats and FMT-processed rats (Fig. 4c-d). Similarly, DEICODE-generated biplots of serum metabolomics (**Fig. S4a**) showed differentiation of SD and FH-SD rats to FH and FH-FH rats (PERMDISP: F-statistic 0.929, p-value 0.382, n = 999 permutations and PERMANOVA: F-statistic 4.907, p-value 0.001, n = 999 permutations), while hippocampus metabolic diversity of SD rats showed distinction with those of the FMT-processed and control FH rats (PERMDISP: F-statistic 1.113, p-value 0.276, n = 999 permutations; PERMANOVA: F-statistic 12.617, p-value 0.001, n = 999 permutations), even though the hippocampal metabolomes of FH-SD rats had the trend toward those of SD rats (**Fig. S4b**). These results indicated that the transplantation of SD gut microbiota to FH rats had a greater effect on the recipients' serum metabolism than hippocampal metabolism. Among the significantly differentially abundant metabolites in control and FMT-processed rats, arachidonic acid (C20:4) in serum was the sole metabolite that was significantly pairwise differentially abundant in FH and FH-FH rats, when compared to SD and FH-SD rats. The abundance of serum C20:4 in FH-SD rats was significantly lower than that in FH-FH rats (Mann-Whitney Wilcox test, p = 0.0007), and was similar to that in the SD donor (p = 0.243). This indicated that the transplantation of SD gut microbiota reduced the serum concentration of C20:4 in FH rats.

Meanwhile, by doing the correlational analyses on the serum and hippocampal metabolomes, respectively, the associative nature of metabolites amongst themselves were identified. Interestingly, it was found that several carbon-rich fatty acids (i.e. palmitic acid (C16:0), heptadecanoic acid (C17:0), stearic acid (C18:0), and linoleic acid (C18:2)) and nitrogen-rich metabolites (e.g. 2-aminoethanol, glucopyranose, glycine, and uracil) had strongly inverse relationships in rat serum (**Fig. S5a**), while numerous nitrogen-rich metabolites (e.g. serine, ornithine, asparagine, and glutamine) had highly negative relationships with several brain osmolyte compounds or their precursors (i.e. N-acetylaspartic acid (NAA), inositol, and pyroglutamic acid) in rat hippocampus (**Fig. S5b**). Considering that the level of C20:4, a derivative of C16:0, C17:0. C18:0, and C18:2 in lipid metabolism, was pairwise significantly reduced in serum of SD and FH-SD rats as shown in Fig. 4A-B, the contents of nitrogen-rich metabolites in serum of SD and FH-SD rats were expected to be higher in comparison with those in FH and FH-FH rats, regardless of the significance, which would result in the increase of amino acids and decrease of osmolytes in the hippocampus through the blood-brain barrier (BBB). This inference was supported by the hippocampal metabolomes of the four groups of rats, where the log ratio of serine to NAA was significantly higher in FH-SD and SD rats than that in FH rats (Mann-Whitney Wilcox test, $p < 0.05$; **Fig. S6**).

To examine the co-occurrences between metabolomes in host tissues and specific bacterial species in gut microbiota, we employed MMvec, which uses neural networks to infer the nature of interactions across omics-datasets. The heatmap reflecting the conditional probabilities between the serum metabolomes and DEICODE-associated and ANCOM-BC-associated bacteria taxa along PC1 (**Fig. S7a**) suggested a strong likelihood of co-occurrence for all pairings with positive and higher conditional probabilities. The model showed a higher predictive accuracy of $Q^2 = 0.35$ than the absolute null or baseline model (where no formula was used) on the cross-validation samples (**Fig. S7b**). Nevertheless, the hippocampal metabolomes did not show good prediction of co-occurrences with the DEICODE-

associated and ANCOM-BC-associated microbes ($Q^2 \approx 0$), hence no visualized data were shown here. This confirmed the expectation that the intestinal microbiome more strongly influenced serum metabolites than hippocampal metabolites.

Discussion

Previous investigations of the gut microbiome and depression have focused on cross-sectional analysis of healthy and depressed subjects[32], or between germ-free and depression-associated microbiome colonized subjects[13]. Our study represents the first to determine if it is possible to alter a depression-like phenotype with fecal microbiota transplants from 'healthy' animals. FMT from SD donors to FH rats, resulted in recipient neurobehaviors more similar to SD rats than FH or FH-FH rats (Fig. 1a-c). Additionally, monoamine neurotransmitter concentrations were significantly increased in the hippocampus (Fig. 1e-g), and three hippocampal immune cytokines (i.e. IL-1b, TNF-α, and IL-17A) were significantly less abundant (**Fig. S1** right panel). A recently similar study in mice demonstrated that gut microbiota from inflammasome NLRP3-deficient mice, whose production of proinflammatory cytokines was limited, ameliorated depressive symptoms in the recipient wild-type mice, but the key gut microbes and their detailed therapeutic mechanism were not investigated[33]. Multi-omics associated analyses on the four groups of rats in the study suggests that FMT directs gut microbiome modulation, and results in systematic metabolic modulation in the recipients through the intestinal mucosal barrier, ENS, and the BBB. We represent this hypothesis in Fig. 5. We characterized the gut microbial community composition of the four groups of rats (Control FH, Control SD, FH-FH, and FH-SD), and found that transplantation of SD fecal microbiota successfully shifted gut microbiomes of the recipient FH rats towards the SD-characteristic microbiome, with a significant reduction in the proportion of several species such as *Dialister* sp. CAG:357 (Fig. 2) and many carbon metabolism-related enzyme-encoding genes such as acetolactate synthase (Fig. 3). With the associated analyses on serum and hippocampus metabolomics profiles (Fig. 4, **Fig. S4, Fig. S5, Fig. S6, Fig. S7**), it was inferred that the significant shift in the gut microbiome of the FH recipients resulted in repression of their carbon metabolism, leading to a reduction in the abundance of carbon-rich metabolites (e.g., C20:4) and an increase in nitrogen-rich metabolites. The increase in nitrogen-rich metabolites in serum may translate to the brain through the BBB, increasing amino acids synthesis in hippocampus (e.g., serine) and decreasing the concentration of brain osmolytes (e.g., NAA). The level of hippocampal NAA has been noted in several human brain disorders[34,35]. Even though its functional roles remain unclear, it is believed to be involved in neuromodulation, which is supported by one interpretation of the results presented here. Alternatively, since depression-biomarkers in the serum of FH-SD rats were not significantly different to that of FH and FH-FH rats (Fig. 1d and **Fig. S1** left panel), and hippocampal metabolites showed no significant co-occurrence with differentially proportional gut microbes, it is possible that transplanted microbes could ameliorate depressive symptoms in recipients by direct neuromodulation through the ENS, potentially via the vagus or other efferent nerves.

The ENS, an intricate network consisting of more than 500 million neuron and glia within the bowel wall, does not only control bowel motility, epithelial secretion, and intestinal immunity[36], but also communicates with the CNS through the vagus and other efferent nerves. Thus, direct stimulation or disruption of the ENS may result in CNS disturbance. Such a mechanism has been proposed for conditions such as Parkinson's disease[37] and Autism Spectrum Disorder[38,39]. The gut microbiome has been associated with direct ENS stimulation and interaction, such as during ENS development in infants[40]. De Vadder et al. found that the germ-free adult mice had immature ENS, and the situation was rescued by gut microbiota from conventionally raised mice, which induced neuronal and mucosal serotonin production and the proliferation of intestine neuronal progenitors[41]. Nevertheless, since the causal relationship between glial bioenergetics and depressive symptoms is not clear yet[42], the detailed mechanisms underpinning such microbiome effects are still hypothetical[43].

In our study, a decreased proportion of *Dialister* sp. CAG:357 was associated with a reduction in depression-like behaviors. *Dialister* spp. are common obligate anaerobes in the human microbiome[44,45], but in conflict with our results, Valles-Colomer et al. found that *Dialister* spp. was consistently depleted in humans with depression[46]. However, this difference could result from differences in the hosts (rat v.s. human), or suggests that *Dialister* is potentially not involved at all in the observed behavioral responses.

In conclusion, we demonstrate that gut microbiota transplantation from 'healthy' SD rats to FH rats can ameliorated depression-like symptoms in the recipients through the gut microbe-induced modulation of host immune and metabolic activity. This study takes a first step toward understanding the potential of FMT as a therapeutic for depression.

Materials And Methods

Animal models

Thirty male Fawn-hooded (FH) rats and ten healthy male Sprague–Dawley (SD) rats at the age of three weeks old and of non-specific pathogen-free (SPF) grade were purchased from Department of Laboratory Animal Science at Peking University Health Science Center (PUHSC). All the rats (n = 40) were pre-housed in cages (i.e., n = 5 rats per cage) for three days in the animal experimental room at PUHSC under SPF conditions for acclimatization. They were housed at 22 ± 1°C with the humidity of 70% on a 12 hour-day: 12 hour-night cycle (lights on 7:00–19:00) and were given standard laboratory chow-diet and water ad libitum.

Fecal microbiota transplantation

From a total of thirty FH rats and ten SD rats, ten FH rats and ten SD rats were used as donors for the fecal microbiota transplantation (FMT) respectively. Fecal pellet samples were collected a day before the FMT experiment and processed as described by Zheng et al.[13]. Briefly, the fecal samples were mixed with sterile phosphate-buffered saline (PBS, pH7.0) at a weight-to-volume ratio of 1:6 under anaerobic

conditions, and then centrifuged at 800 ×g for 2 min to discard the fecal debris. The microbiota in the supernatants were stored overnight at 4°C for the FMT in the following day. The remaining twenty FH rats were divided into two equal-sized groups based on equivalent average body weight. The fecal extracts from the FH and SD donor rats were administered to the first group named as 'FH-FH' and the second group named as 'FH-SD' rats respectively. Each inoculation volume was of 0.5 mL performed at a total of eight times around a single-day interval. In parallel to these experimental groups, an additional control group of ten FH rats and ten SD rats were treated with PBS under the same incubation conditions.

Neurobehavioral tests

Animal model rats were examined for their neurobehaviors using the following commonly conducted behavioral tests: forced swim test (FST), open-field test (OFT), and sucrose preference test (SPT). Each test was performed post-FMT in the animal experimental room at PUHSC in three separate days with prior acclimation for one hour. The details of the testing operations are as follows:

1. Forced swim test: The FST was carried out according to Ge et al.[47]. The rats were placed individually in a PVC-made translucent cylinder (50 cm in height × 20 cm in diameter) filled with 30 cm water (22.5 ± 0.5°C), in which the rats could not support themselves touching the bottom with their bodies. The testing paradigm included two sections: an initial 15-minute pre-test for acclimation, and then 5-minute test 24 hours later. A video camera was held near the cylinder to record the duration of the rat's immobile state in the second section. Immobility was defined such that all motions of the rat limbs stroke was absent except for movements required to keep the rat's head above water.

2. Open field test: All the rats were individually tested in an open-field apparatus consisting of a grey square base (100 × 100 cm^2) with grey walls (40 cm in height), made up of polyvinyl chloride (PVC). Each rat was gently placed in the center of the chamber, and its spontaneous activity was recorded for 10 minutes using the video-computerized tracking system, which was set at 100 cm above the chamber. For recording purposes, the base area was equally arranged into 5×5 squares, and the value of the total square amounts in which the experimental rat set foot during the 10-minute testing was used as an index of locomotor activity, while the proportion of central squares (inner 36% of the base area) to the total squares in which the experimental rat set foot during the 10-minute testing was construed as an index of anxiety-like behavior. The chamber was cleaned up before the next rat was placed in.

3. Sucrose preference test: Two no-drip pet water feeding bottles containing 1.0% (w/v) sucrose were hung on different sides of the experimental cage. Before conducting the experiment, rats were mono housed in the experimental cage with the provision of two water bottles for 48 hours to overcome neophobia. And, followed by an exposure to a six-hour period of water and food deprivation. Next, the solutions in the two bottles were each replaced with 80mL of 1% sucrose and plain water, respectively. Each experimental rat was provided with an open access to the two bottles hanging on each side of the cage for 30-minutes. Later, the sucrose and plain water bottles were switched, and the open access was provided for another 30-minutes, to eliminate side-preference artifacts. Each of the bottles was weighed before and after use. The sucrose preference index of each rat was computed according to the following formula:

$$I_{SP} = \frac{\Delta M_s}{\Delta M_s + \Delta M_w} \times 100\%$$

where I_{SP} is the sucrose preference index of each rat, ΔM_s is the weight difference of the sucrose bottle before and after SPT, and ΔM_w is the weight difference of the water bottle before and after SPT.

Extraction of neurotransmitters, immune cytokines and metabolites from the hippocampal tissues and serum

One-week post FMT, the control and experimental rats were sacrificed to obtain the hippocampal and serum samples. The hippocampal tissue from each rat was divided into two aliquots, one for sample preparation and quantification of neurotransmitters and immune cytokines, and the other one for sample preparation and quantification of untargeted metabolomics.

Sample preparation for neurotransmitters and immune cytokines was processed as follows: the hippocampal tissue was weighed and homogenized in the lysis buffer (composition consists of 10 mM HCl, 1 mM EDTA, 4 mM $Na_2S_2O_5$) to a ratio of 6 mL lysis buffer to 1 mg tissue sample. Then, the mixed homogenate was centrifuged at 12,000 rpm and 4°C for 10 min. The supernatant was filtered using 0.2 μm Millipore filter (Millipore, Ireland), and stored at -80°C until further use.

Sample preparation for metabolomics was processed as follows: The hippocampal tissue was desalinated using methanol, i.e., 20 mg of the hippocampus tissue was mixed with 800 mL methanol-water (4:1 v/v) solution containing 5 μg mL^{-1} myristic acid-1,2-$^{13}C_2$, which was used as the internal standard for the metabolomics. This mixture was further milled using the rotor beater mill (Retsch, Germany) three times, and then incubated at 4°C for 60 minutes followed by centrifugation at 20,000 ×g and 4°C for 10 min. The supernatant was filtered using 0.2 μm Millipore filter (Millipore, Ireland), and stored at -80°C until further derivatization and analysis. 120 μL of the desalinated hippocampal extract was added to a MS certified glass-vial equipped with a 200 μL insert (Freeze-Dryer, Boyikang, Beijing, China) for four hours of lyophilization. This lyophilized material was derivatized using a method analogous to Moros et al.[48], where the lyophilized samples were mixed with 30 μL methoxyamine (10 mg mL^{-1}) in pyridine for 16 hours at room temperature for the methoxyamination, followed by the trimethylsilylation with 30 μL of N-methyl-N-(trimethylsilyl) trifluoroacetamide (MSTFA) with 1% trimethylchlorosilane (TMCS). Subsequently, 30 μL of methyl myristate in *n*-pentadecane was added as an injection external standard.

For serum metabolomics, 50 μg of fresh serum sample was extracted with 200 μL of cold methanol-water solution containing the internal standard myristic acid-1,2-$^{13}C_2$. Later, the mixture was centrifuged, lyophilized, and derivatized in a similar method to that used for hippocampal samples (as described above).

ELISA-based quantification of neurotransmitters in the hippocampus and serum

Absolute quantification of 5-hydroxytryptamine in the hippocampal-tissue- and serum-extracts was determined using the serotonin-specific enzyme-linked immunosorbent assay (ELISA) kit DEE5900 and DEE8900 (Demeditec Diagnostics GmbH, Kiel, Germany) respectively. The concentration of dopamine and noradrenaline (NE) in the hippocampal-tissue- and serum-extracts were both determined with the dopamine-specific and noradrenaline-sensitive ELISA assay kit BCU39-K01 (Eagle Biosciences Inc., Amherst, NH, USA). All the samples were run in 3 biological replicates on each ELISA microplate.

GC-MS-based quantification of host and microbial metabolites in the hippocampus and serum

Metabolite profiling of the derivatized samples were performed on a GCMS-QP2010 (SHIMADZU, Japan). A 0.5 µL of the derivatized sample was injected into a RTx-5MS column (30 m × 0.25 mm × 0.25µm, Restek Corp., PA, USA) with helium as carrier gas at a constant flow of 1.5 mL min^{-1}. The inlet temperature was set to be 250ºC. The initial oven temperature was held at 80ºC, ramped to 300ºC by 20ºC $minute^{-1}$, and then held at 300 ºC for 3 minutes. Electron impact was used as an ionization source with the ionization energy of 70 eV at 200 ºC. The transfer line temperature was set to be 220 ºC. Mass spectra were recorded at 50–700 m/z for 4.5–18 min. Metabolites were identified based on the mass spectrum in comparison to the standard NIST library 2.0 (National Institute of Standards and Technology, 2008) and Wiley 9 (Wiley-VCH Verlag GmbH & Co. KgaA, Weinheim, Germany), with a threshold of match > 80 (with a maximum match equal to 100). Relative metabolite abundances were calculated from peak areas (unique mass) of identified metabolites using GCMS LabSolution software and followed by calibration using the peak area of the internal standard (myristic acid-1,2-$^{13}C_2$) and the external standard (methyl myristate) to minimize the instrumental errors.

AimPlex multiplex immunoassays-based quantification of cytokines in the hippocampus and serum

To detect the immune cytokines in rat hippocampus and serum, an AimPlex multiplex immunoassay kit (Beijing Quantobio, China) was used according to the manufacturer's instruction. This assay combined the techniques in ELISA and high-throughput flow cytometry and could detect several proteins from very little samples quickly. Here, eight inflammatory cytokines were measured, including IL-4, IL-10, TNF-α, IL-1b, IL-2, IL-6, IL-17A, and IFN-α.

Nucleic-acid extraction and sequencing

One-week post FMT, fecal samples were collected from the control and experimental rats and were processed for 16S rRNA amplicon sequencing and shotgun metagenomic sequencing. DNA extraction for amplicon-based sequencing was processed using the QIAamp Fast DNA Stool Mini Kit (QIAGEN, Duesseldorf, Germany) to extract the microbial genomic DNA. The V3-V4 region of the 16S rRNA gene was PCR-amplified from the DNA samples using the universal primer 338F (5'-ACTCCTACGGGAGGCAGCA-3') and 806R (5'-GGACTACHVGGGTWTCTAAT-3') for Illumina HiSeq paired-end sequencing. DNA extraction for shotgun-based sequencing was processed using the NEBNext®

Ultra™ DNA Library Prep Kit (NEB, USA) to build the sequencing library from a total amount of 1μg DNA per sample. The generated library was sequenced on Illumina HiSeq2500 platform.

Analysis of 16S rRNA sequencing

Demultiplexed sequencing data was quality filtered by trimming to 150 bases and were denoised using Deblur[49] through Qiita[50] using the default to generate amplicon sequencing variants (ASVs). The deblurred sequence fragments were inserted into the Greengenes Database (v.13_8) phylogenetic tree using SATé-enabled phylogenetic placement[51]. The final feature table obtained from Qiita is composed of 37 samples and 7,467 features. Rarefied data table of 5,000 reads per sample was employed for performing downstream data analyses using QIIME2[52].

Analysis of shotgun sequencing

Quality control-filtered paired-end sequencing reads were then concatenated, converted to fasta format, and processed by the SHOGUN align function[53] and associated Web of Life phylogenetic database[54]. SHOGUN-aligned files were then utilized by Woltka (https://github.com/qiyunzhu/woltka) for gOTU table generation and functional pathway characterization on a per-sample basis. This tool maps sequencing reads to microbial genes based on their associated genomic coordinates to compute microbial functional units (e.g., MetaCyc pathways, protein, enzyme, reaction, and pathway information[55]). In doing so, it avoids the microbial functional profiling based on the presence or absence of predefined marker genes. The gOTU table was filtered to remove microbial features per sample with less than 0.001% of relative abundance, leaving 1,543 out of 5,842 gOTUs (with the rank-none parameter) and leaving 894 out of 3,325 gOTUs (with the rank-free parameter) found across all samples. The raw sequencing data were deposited in the National Microbiology Data Center (NMDC) under the accession numbers of NMDC10017888.

Statistical analysis and visualization

The feature abundance table generated from Qiita (taxonomic assignments) and Woltka (functional assignments) was used as input for beta-diversity Robust Aitchison PCA (using DEICODE) to calculate between-group beta diversity in QIIME2[56]. The beta diversity significance within and among groups was examined by QIIME2 diversity plugin with PERMDISP and PERMANOVA tests. The resulting PCoA and the biplots were visualized using the QIIME2 plugin Emperor[57]. Distance matrices used for between-group differences were tested using PERMANOVA and permuted t tests in QIIME2. The feature loadings in the biplot axis with the most difference in groups were visualized using Qurro[58]. The abundance of the highest- and lowest-ranked features were used to compute log-ratios in different rat groups. ANCOM-BC was used to calculate the pairwise differential species[59]. To estimate the conditional probability of a metabolite abundance given the presence of a single microbe, a log-transformed conditional probability matrix from each cross-omics feature pair i.e., metagenomics (based on the species-level metagenomic data) and metabolomics was built using a neural network algorithm MMvec[60]. The GC-MS metabolomics data was filtered for central carbon metabolites in the hippocampal tissue and serum extract. For non-

parametric distributed data, Wilcoxon signed-rank and Kruskal-Wallis were used to assess the diversity between two or multiple groups respectively.

Declarations

Acknowledgement

This work was supported by the National Key R&D Program of China (2018YFA0902100 to XW; 2020YFA0908300 to BH), Open Funding Project of the State Key Laboratory of Biochemical Engineering (No. 2020KF-05), and the Beijing Institute of Technology Research Fund Program for Young Scholars.

Author contributions

Conceptualization, Nie, Y. and Wu, X.; Methodology, Hu, B., Das, P. and Lv, X.; Validation, Hu, B. and Lv, X.; Formal analysis, Das, P.; Investigation, Hu, B., Das, P., and Lv, X.; Resources, Shi, M. and Aa, J.; Data curation, Hu, B. and Lv, X.; Visualization, Das, P. and Hu, B.; Writing-original draft preparation, Hu, B. and Das, P.; Wring-review & editing, Gilbert, J., Wang, K., Duan, L. and Nie, Y.; Project administration, Nie, Y. and Wu, X.; Funding Acquisition, Hu, B. and Wu, X.

Competing interests statement

The authors declare no conflict of interest.

Ethics statement

The protocols of animal experimentation were approved by the Committee on the Ethics of Animal Experiments of Peking University Health Science Center with the approval number of LA2015214.

References

1. WHO. FIFA launches #ReachOut campaign for better mental health. https://www.who.int/news/item/02-08-2021-fifa-launches-reachout-campaign-for-better-mental-health (2021).
2. Stetler, C. & Miller, G. E. Depression and hypothalamic-pituitary-adrenal activation: a quantitative summary of four decades of research. *Psychosom Med* **73**(2), 114–126 (2011).
3. Boku, S., Nakagawa, S., Toda, H. & Hishimoto, A. Neural basis of major depressive disorder: beyond monoamine hypothesis. *Psychiatry Clin Neurosci* **72**(1), 3–12 (2018).
4. Leonard, B.E. Inflammation and depression: a causal or coincidental link to the pathophysiology? *Acta Neuropsychiatr* **30**(1), 1–16 (2018).
5. Foster, J.A. & McVey Neufeld, K. Gut-brain axis: how the microbiome influences anxiety and depression. *Trends Neurosci* **36**(5), 305–312 (2013).

6. Goyal, M.S., Venkatesh, S., Mibrandt, J., Gordon, J.I. & Raichle, M.E. Feeding the brain and nurturing the mind: linking nutrition and the gut microbiota to brain development. *Proc Natl Acad Sci U S A* **112**(46), 14105–14112 (2015).
7. Cryan, J.F. et al. The microbiota-gut-brain axis. *Physiol Rev* **99**(4), 1877–2013 (2019).
8. Jiang, H. et al. Alter fecal microbiota composition in patients with major depressive disorder. *Brain Behav Immun* **48**, 186–194 (2015).
9. Strandwitz, P. et al. GABA-modulating bacteria of the human gut microbiota. *Nat Microbiol* **4**, 396–403 (2019).
10. Averina, O.V. et al. Bacterial metabolites of human gut microbiota correlating with depression. *Int J Mol Sci* **21**(23), 9234 (2020).
11. Zheng, P. et al. The gut microbiome modulates gut-brain axis glycerophospholipid metabolism in a region-specific manner in a nonhuman primate model of depression. *Mol Psychiatry* https://doi.org/10.1038/s41380-020-0744-2 (2020).
12. Tillmann, S., Abildgaard, A., Winther, G. & Wegener, G. Altered fecal microbiota composition in the Flinders sensitive line rat model of depression. *Psychopharmacology (Berl)* **236**(5), 1445–1457 (2019).
13. Zheng, P. et al. Gut microbiome remodeling induces depressive-like behaviors through a pathway mediated by the host's metabolism. *Mol Psychiatry* **21**(6), 786–796 (2016).
14. Kelly, J. R. et al. Transferring the blues: depression-associated gut microbiota induces neurobehavioural changes in the rats. *J Psychiatr Res* **82**, 109–118 (2016).
15. Hsiao, E.Y. et al. Microbiota modulate behavioral and physiological abnormalities associated with neurodevelopmental disorders. *Cell* **155**(7), 1451–1463 (2013).
16. Dinan, T.G., Stilling, R.M., Stanton, C. & Cryan, J.F. Collective unconscious: how gut microbes shape human behavior. *J Psychiatr Res* **63**, 1–9 (2015).
17. Mao, R. et al. Different levels of pro- and anti-inflammatory cytokines in patients with unipolar and bipolar depression. *J Affect Disord* **237**, 65–72 (2018).
18. Obrenovich, M.E.M. Leaky gut, leaky brain. *Microorganisms* **6**(4), e107 (2018).
19. El Aidy, S., Dinan, T.G. & Cryan, J.F. Immune modulation of the brain-gut-microbe axis. *Front Microbiol* **5**, 146 (2014).
20. Mawe, G.M. & Hoffman, J.M. Serotonin signalling in the gut—functions, dysfunctions and therapeutic targets. *Nat Rev Gastroenterol Hepatol* **10**(8), 473–486 (2013).
21. Rudzki, L. & Maes, M. The microbiota-gut-immune-glia (MGIG) axis in major depression. *Mol Neurobiol* **57**(10), 4269–4295 (2020).
22. Rutsch, A., Kantsjö, J.B. & Ronchi, F. Inflammasome influence brain physiology and pathology. *Front Immunol* **11**, 604179 (2020).
23. Liu, R.T., Walsh, R.F.L. & Sheehan, A.E. Prebiotics and probiotics for depression and anxiety: a systematic review and meta-analysis of controlled clinical trials. *Neurosci Biobehav Rev* **102**, 13–23

(2019).

24. Bear, T.L.K. et al. The role of the gut microbiota in dietary interventions for depression an anxiety. *Adv Nutr* **11**(4), 890–907 (2020).
25. Pinto-Sanchez, M. I. et al. Probiotic *Bifidobacterium longum* NCC3001 reduces depression scores and alters brain activity: a pilot study in patients with irritable bowel syndrome. *Gastroenterology* **153**(2), 448–459 (2017).
26. Hao, Z., Wang, W., Guo, R. & Liu, H. *Faecalibacterium prausnitzii* (ATCC 27766) has preventive and therapeutic effects on chronic unpredictable mild stress-induced depression-like and anxiety-like behavior in rats. *Psychoneuroendocrinology* **104**, 132–142 (2019).
27. Östlund-Lagerström, L. et al. Probiotic administration among free-living older adults: a double blinded, randomized, placebo-controlled clinical trial. *Nutr J* **15**(1), 80 (2016).
28. Lozupone, C.A., Stombaugh, J.I., Gordon, J.I., Jansson, J.K. & Knight, R. Diversity, stability and resilience of the human gut microbiota. *Nature* **489**, 220–230 (2012).
29. Peirce, J.M. & Alviña, K. The role of inflammation and the gut microbiome in depression and anxiety. *J Neurosci Res* **97**(10), 1223–1241 (2019).
30. Li, N. et al. Spatial heterogeneity of bacterial colonization across different gut segments following inter-species microbiota transplantation. *Microbiome* **8**, 161 (2020).
31. Knapp, D.J., Harper, K.M., Melton, J. & Breese, G. Comparative effects of stressors on behavioral and neuroimmune responses of fawn-hooded (FH/Wjd) and Wistar rats: Implications for models of depression. *J Neuroimmunol* **322**, 74–80 (2018).
32. Huang, T. et al. Current understanding of gut microbiota in mood disorders: an update of human studies. *Front Genet* **10**, 98 (2019).
33. Zhang, Y. et al. Gut microbiota from NLRP3-deficient mice ameliorates depressive-like behaviors by regulating astrocyte dysfunction via circHIPK2. *Microbiome* 7: 116 (2019).
34. Rael, L.T., Thomas, G.W., Bar-Or, R., Craun, M.L. & Bar-Or, D. An anti-inflammatory role for N-acetly aspartate in stimulated human astroglial cells. *Biochem Biophys Res Commun* **319**, 847–853 (2004).
35. Warepam, M. et al. N-acetylaspartate is an important brain osmolyte. *Biomolecules* **10**(2), 286 (2020).
36. Schneider, S., Wright, C.M. & Heuckeroth, R.O. Unexpected roles for the second brain: enteric nervous system as master regulator of bowel function. *Annu Rev Physiol* **81**, 12.1-12.25 (2019).
37. Pan-Montojo, F. et al. Progression of Parkinson's disease pathology is reproduced by intragastric administration of rotenone in mice. *PLoS One* **5**(1), e8762 (2010).
38. Bernier, R. et al. Disruptive CHD8 mutations define a subtype of autism early in development. *Cell* **158**, 263–76 (2014).
39. Grubišić, V., Kennedy, A., Sweatt, J.D. & Parpura, V. Pitt-Hopkins mouse model has altered particular gastrointestinal transits *in vivo*. *Autism Res* **8**(5), 629–633 (2015).

40. Lu, J. et al. Effects of intestinal microbiota on brain development in humanized gnotobiotic mice. *Sci Rep* **8**, 5443 (2018).
41. De Vadder, F. et al. Gut microbiota regulates maturation of the adult enteric nervous system via enteric serotonin networks. *Proc Natl Acad Sci U S A* **115**(25), 6458–6463 (2018).
42. Wang, Q., Jie, W., Liu, J., Yang, J. & Gao, T. An astroglial basis of major depressive disorder? An overview. *Glia* **65**, 1227–1250 (2017).
43. Heiss, C.N. & Olofsson, L.E. The role of the gut microbiota in development, function and disorders of the central nervous system and the enteric nervous system. *J Neuroendocrinol* **31**(5), e12684 (2019).
44. Sakamoto, M. et al. *Dialister hominis* sp. nov., isolated from human faeces. *Int J Syst Evol Microbiol* **70**(1), 589–595 (2020).
45. Afouda, P., Dubourg, G., Tomeï, E., Raoult, D. & Fournier, P.E. *Dialister massiliensis* sp. nov., a new bacterium isolated from the human gut. *New Microbes New Infect* **34**, 100657 (2020).
46. Valles-Colomer, M. et al. The neuroactive potential of the human gut microbiota in quality of life and depression. *Nat Microbiol* **4**(4), 623–632 (2019).
47. Ge, J., Peng, Y., Qi, C., Chen, F. & Zhou, J. Depression-like behavior in subclinical hypothyroidism rat induced by hemi-thyroid electrocauterization. *Endocrine* **45**(3), 430–8 (2014).
48. Moros, G., Chatziioannous, A.C., Gika, H.G., Raikos, N. & Theodoridis, G. Investigation of the derivatization conditions for GC-MS metabolomics of biological samples. *Bioanalysis* **9**(1), 53–65 (2017).
49. Nearing, J.T., Douglas, G.M., Comeau, A.M. & Langille, M.G.I. Denoising the denoisers: an independent evaluation of microbiome sequence error-correction approaches. *Peer J* **6**, e5364 (2018).
50. Gonzalez, A. et al. Qitta: rapid, web-enabled microbiome meta-analysis. *Nat Methods* **15**(10), 796–798 (2018).
51. Mirarab, S., Nguyen, N. & Warnow, T. SEPP: SATe-enable phylogenetic placement. *Pac Symp Biocomput* **2012**, 247–258 (2012).
52. Hall, M. & Beiko, R.G. 16S rRNA gene analysis with QIIME2. *Methods Mol Biol* **1849**, 113–129 (2018).
53. Hillmann, B. et al. SHOGUN: a modular, accurate and scalable framework for microbiome quantification. *Bioinformatics* **36**(13), 4088–4090 (2020).
54. Zhu, Q. et al. Phylogenomics of 10,575 genomes reveals evolutionary proximity between domains Bacteria and Archaea. *Nat Commun* **10**, 5477 (2019).
55. Caspi, R. et al. The MetaCyc database of metabolic pathways and enzymes. *Nucleic Acids Res* **46**(D1), D633-D639 (2018).
56. Martino, C. et al. A novel sparse compositional technique reveals microbial perturbations. *mSystems* **4**(1), e00016-19 (2019).
57. Vázquez-Baeza, Y., Pirrung, M., Gonzalez, A. & Knight, R. EMPeror: a tool for visualizing high-throughput microbial community data. *Gigascience* **2**(1), 16 (2013).

58. Fedarko, M.W. et al. Visualizing 'omics feature rankings and log-ratios using Qurro. *NAR Genom Bioinform* **2**(2), lqaa023 (2020).

59. Lin, H. & Peddada, S.D. Analysis of compositions of microbiomes with bias correction. *Nat Commun* **11**, 3514 (2020).

60. Morton, J.T. et al. Learning representations of microbe-metabolite interactions. *Nat Methods* **16**(12), 1306–1314 (2019).

Figures

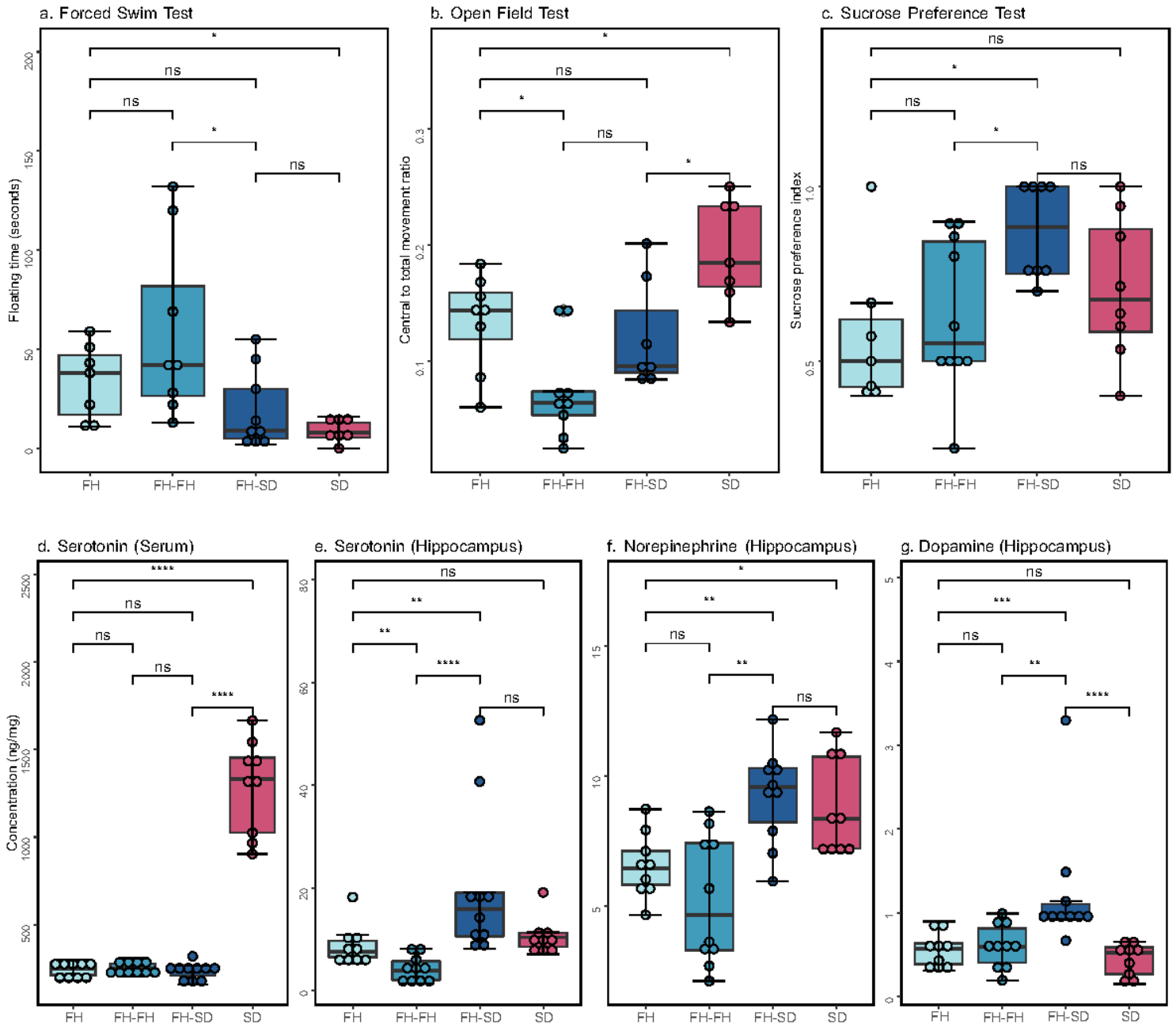

Figure 1

Physiological characterization of neurobehavioral, and neurotransmitters. Boxplots showing the test scores of forced swim test (a), open field test (b), and sucrose preference test (c), concentration of serotonin in serum (d), and concentrations of serotonin, norepinephrine, and dopamine in hippocampus (e-g). The asterisks indicate as follows: ns, $p > 0.05$; *, $p \leq 0.05$; **, $p \leq 0.01$; ***, $p \leq 0.001$; ****, $p \leq 0.0001$ (t-test).

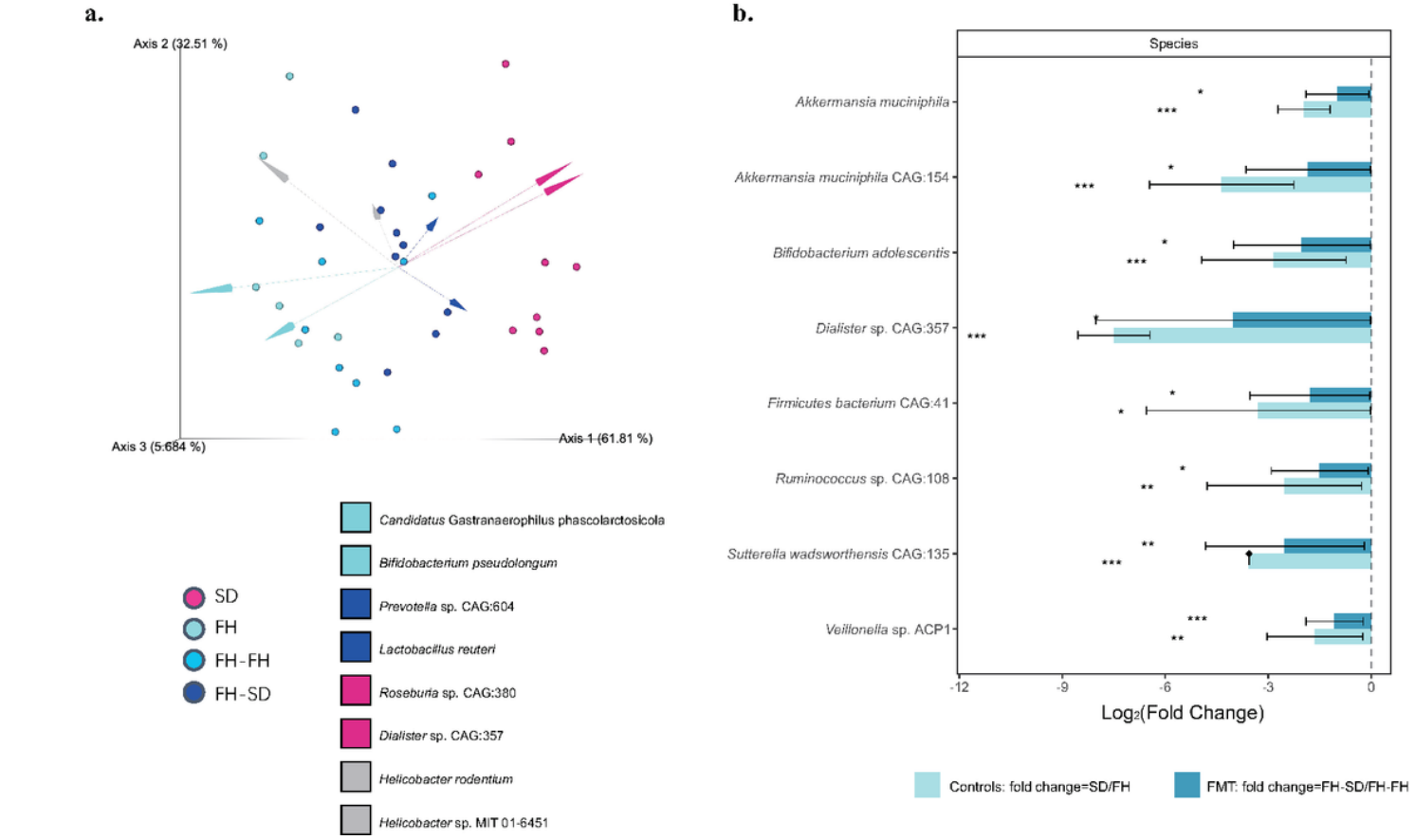

Figure 2

Quantitative analysis of gut microbial diversity and proportions. (a) DEICODE (robust Aitchison PCA) generated biplot. Data points represent individual rats and are colored by group. Taxa driving the ordination space are exemplified by the vectors, labeled with the lowest common ancestor. (b) ANCOM-BC model-derived pairwise differential proportion analysis stratified by control and FMT groups where the data is represented by effect size (log fold change) and 95% confidence interval bars (two-sided; Bonferroni adjusted). All effect sizes with adjusted $p < 0.05$ are indicated: *, significant at 5% level of significance; **, significant at 1% level of significance; ***, significant at 0.1% level of significance.

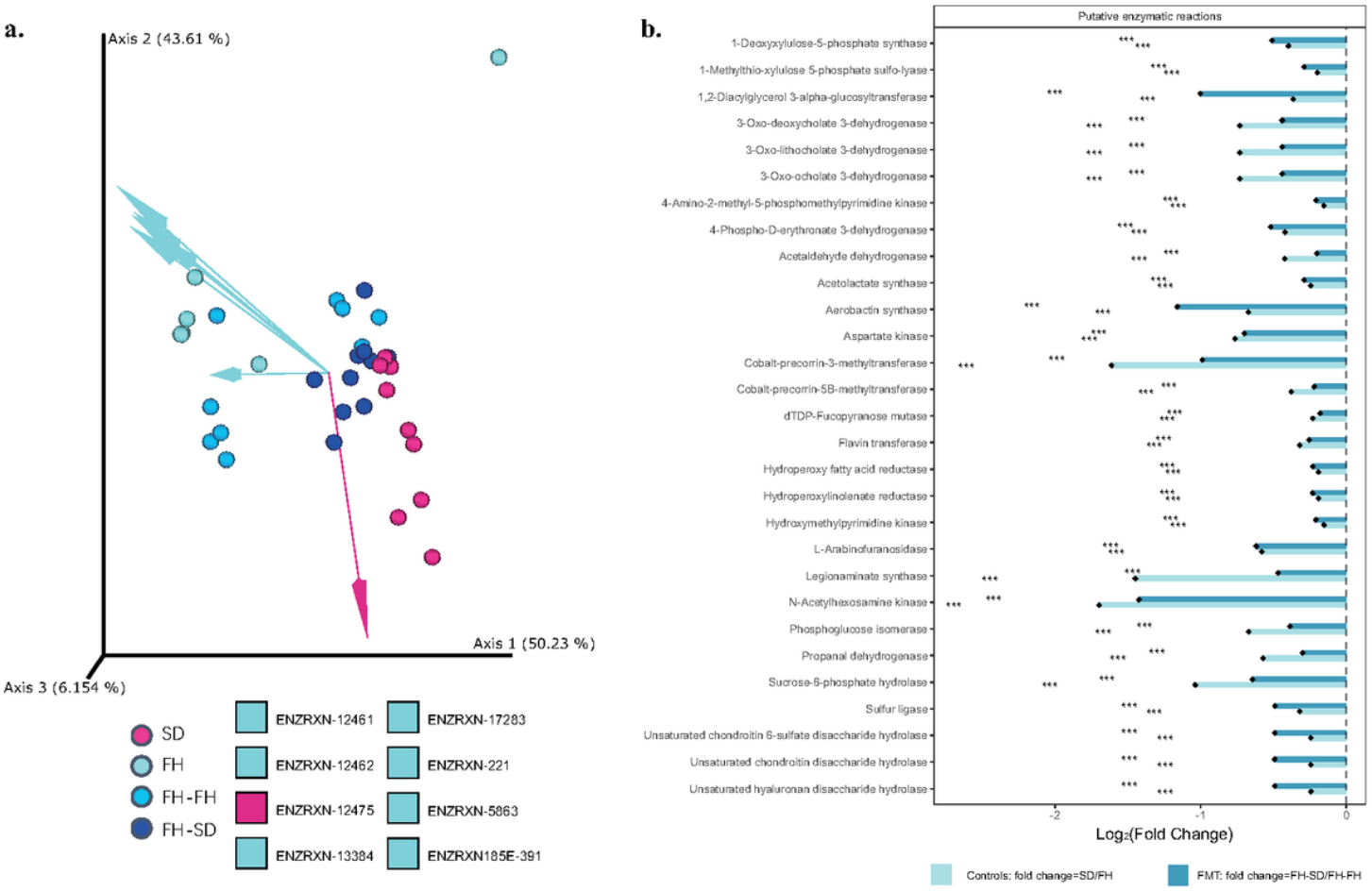

Figure 3

Quantitative analysis of gut functional diversity and abundance in terms of enzymatic reactions. (a) DEICODE (robust Aitchison PCA) generated biplot of enzyme reactions. Data points represent individual rats and are colored by group, and arrows represent enzymatic genes. ENZRXN-12461, citrate hydro-lyase; ENZRXN-12462m D-threo-isocitrate hydro-lyase; ENZRXN-12475, 1-deoxy-D-xylulose 5-phosphate reductoisomerase; ENZRXN-13384, sucrose phosphorylase; ENZRXN-17263, acetolactate synthase; ENZRXN-221, butyryl-CoA dehydrogenase; ENZRXN-5863, isoamylase; ENZRXN-185E-391, phosphoglucomutase. (b) ANCOM-BC model-derived pairwise differential proportion analysis on enzymatic genes stratified by control and FMT groups, where the data is represented by effect size (log (fold change)) and 95% confidence interval bars (two-sided; Bonferroni adjusted). Diamonds on top of some bars indicate structural zeros. All effect sizes with adjusted $p < 0.05$ are indicated as follows: *, significant at 5% level of significance; **, significant at 1% level of significance; ***, significant at 0.1% level of significance.

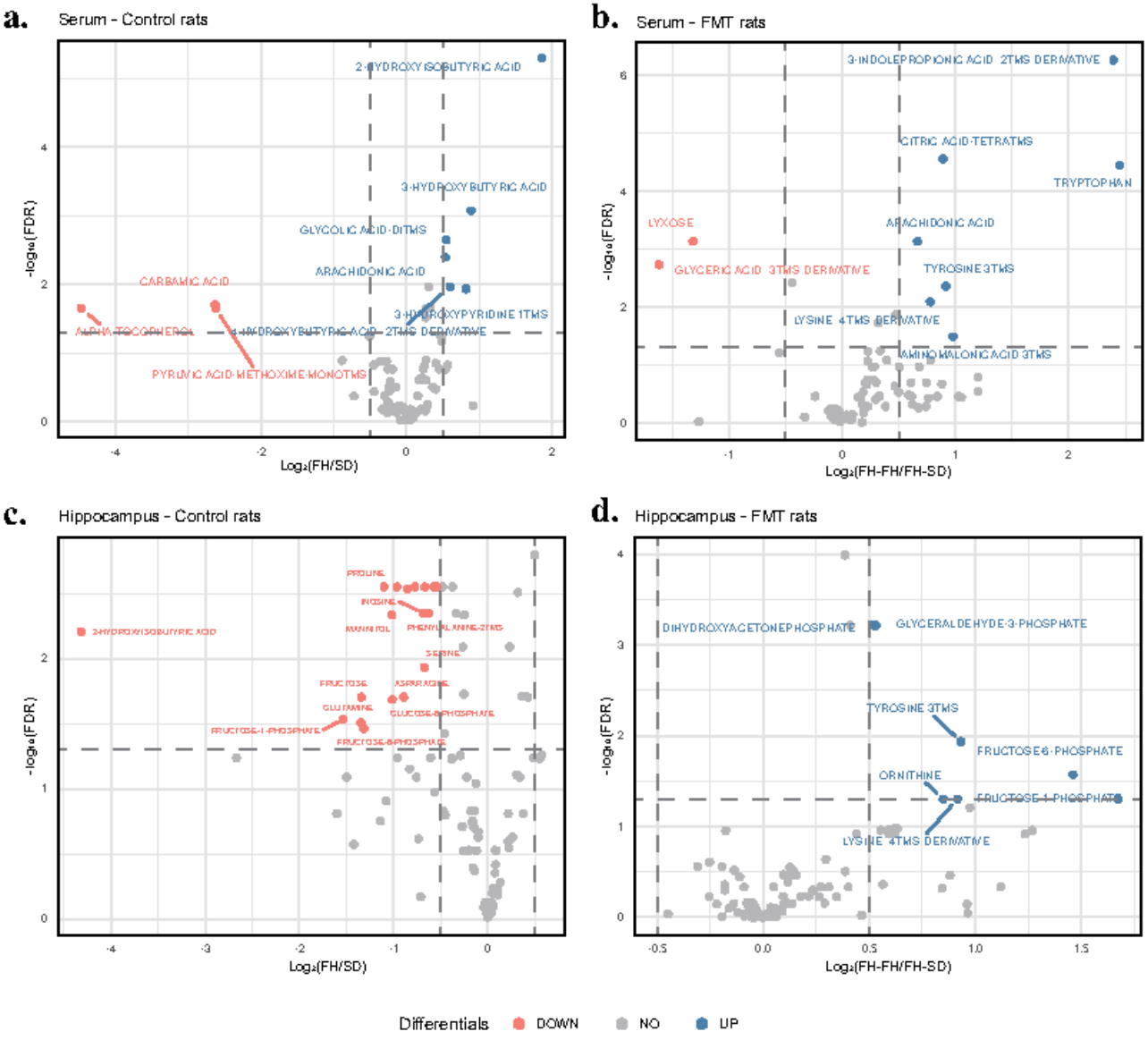

Figure 4

Volcano plots showing the differential metabolites in serum and hippocampal tissues. Log2(fold change) > 0.5, FDR value < 0.05 (in blue): significantly higher in FH rats than that in SD rats (control rats) or in FH-FH rats than that in FH-SD rats (FMT rats), respectively; Log2FC < 0.5, FDR value < 0.05 (in red): significantly reduced in FH rats than that in SD rats (control rats) or in FH-FH rats than that in FH-SD rats (FMT rats), respectively.

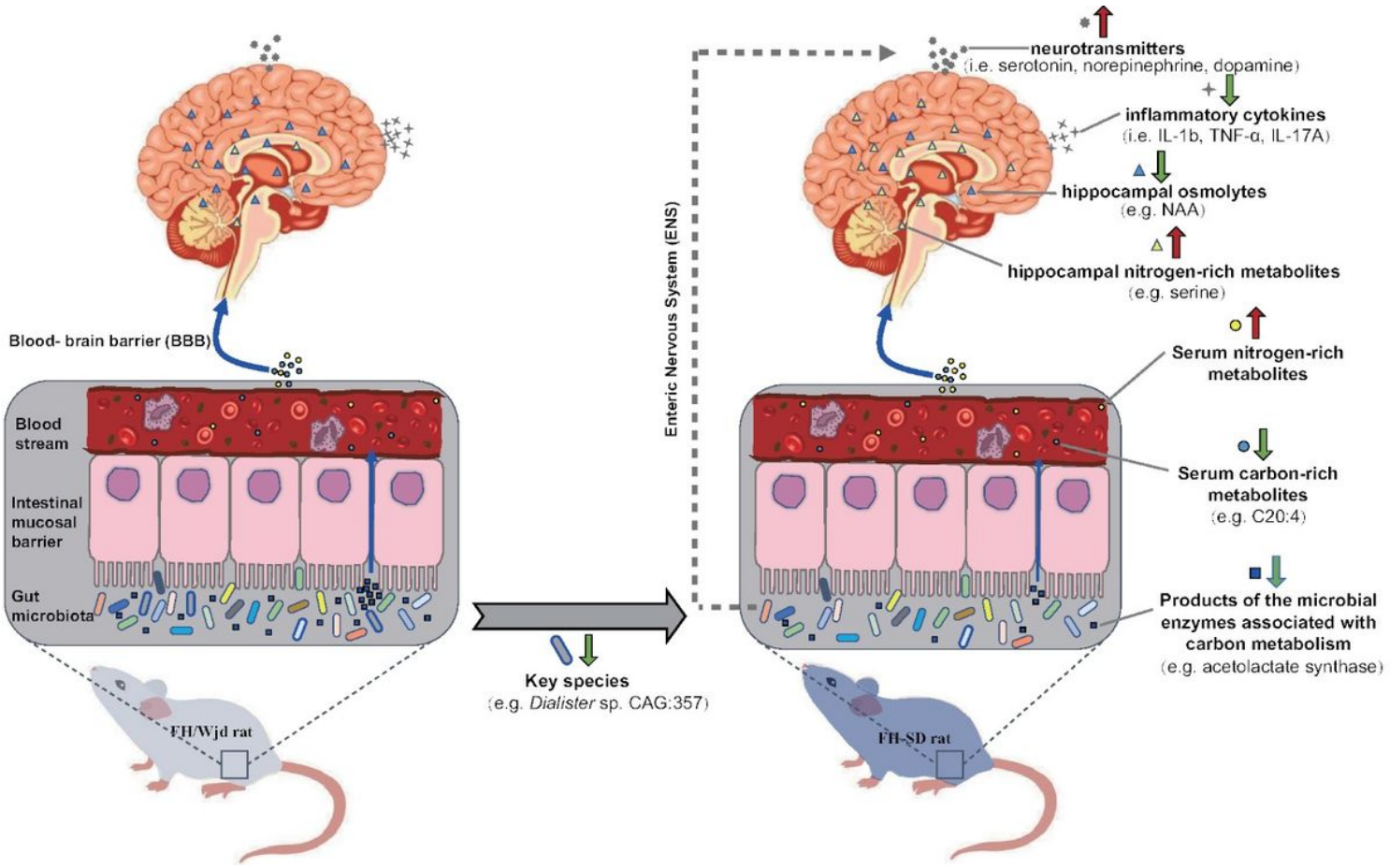

Figure 5

A predicted mechanistic overview for the potential therapeutic impact of FMT resulting in a reduction in depression-like behaviors in recipient hosts. The cobalt blue arrows represent the effect of gut microbiota on neurogenesis and hippocampal inflammation through the blood-brain barrier (BBB); the dotted gray arrow represents potential effects of the gut microbiota on neurogenesis directly through the enteric nervous system (ENS). Compounds in different tissues are represented by different geometric shapes. The thick red and green arrows represent the increasing and decreasing levels of the responding objects, respectively. C20:4 = arachidonic acid; NAA = N-acetylaspartic acid.

Supplementary Files

This is a list of supplementary files associated with this preprint. Click to download.

- Supplementaryfiles.docx